Nitrogen Bis-Phosphonate-passivated γFe_2O_3 nanoparticles: nanovectors with antiproliferative activity

Farah Benyettou*, Yoann Lalatonne**, Odile Sainte-Catherine*, Nicole Lièvre, Marc Lecouvey*, Laurence Motte****

[*] *Laboratoire CSPBAT FRE 3043 CNRS, Pr Laurence Motte*
Université Paris 13, 74 Rue Marcel Cachin 93017 Bobigny, France. Fax: (+) 01.48.38.76.25. E-mail: laurence.motte@smbh.univ-paris13.fr
[**] *Service de Médecine Nucléaire, Hôpital Avicenne, Route de Stalingrad 93009 Bobigny, France.*
[***] *UPRES 3410 Biothérapies Bénéfices et risques, 74 rue Marcel Cachin 93017 Bobigny, France.*

ABSTRACT

A magnetic nanovector is elaborated to vectorize Bisphosphonates (BPs), anticancer interest molecules. The anchoring to the nanoparticle's surface allowed to increase their hydrophobicity and also to change the therapeutic target, increasing the BPs intestinal absorption instead of their accumulation in bone. We show that BPs link to the nanoparticle surface through phosphonate groups. The biological *in-vitro* tests performed on breast cancer cell line, MDA-MB 231, showed that γFe_2O_3@BPs have antiproliferative activity. In addition, the γFe_2O_3 core could be used as MRI contrast agent for a good therapeutic evaluation.

Keywords: Drug nanoparticle, Magnetic nanoparticle, Bisphosphonate, Cancer drugs, Drug targeting, Cell internalization

BPs are widely used as inhibitors of bone resorption, such as osteoporosis, solid tumour bone metastases and myeloma bone disease.[1,2] They are analogues of the naturally occurring inorganic pyrophosphate in which P-O-P linkage has been replaced by a non hydrolysable P-C-P bond. The R_1 and R_2 carbon side chains determine the pharmacological properties of bisphosphonates. BPs acts as powerful pharmacological agents with the ability to inhibit osteoclast activity, influence cellular processes involved in bone formation and resorption activity, induce osteoclast apoptosis in vitro and in vivo and reduce biochemical markers of bone resorption[3]. Most BPs contain a hydroxyl group at the R_1 position position (HMBP hydroxyl methylene bisphosphonate) that confers high affinity binding to calcium phosphate (hydroxyapatite ($Ca_{10}(PO_4)_6(OH)_2$) and is the basis for the bone targeting properties of bisphosphonates[4,5]. The R_2 side chain is the essential determinant of antiresorptive potency (osteoclasts inhibition). Nonnitrogen-containing compounds are metabolized into cytotoxic analogues of ATP, whereas the more potent nitrogen-containing compounds (N-BPs; e.g., pamidronate, Alendronate, ibandronate, Zoledronate) (scheme 1) inhibit protein prenylation, thus affecting cell function and survival[5]. Zoledronate and Alendronate are mainly used clinically in prevention of skeletal complications in patients with advanced bone affecting malignant tumours.

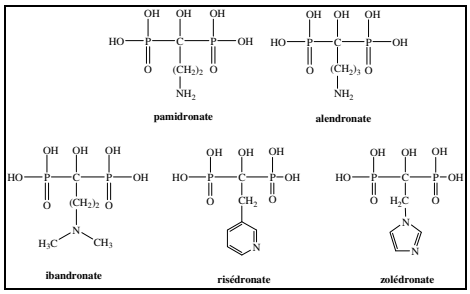

Scheme 1: General chemical structure of the most important N-BPs clinically used

In addition, Zoledronate and Alendronate also exhibit direct and indirect antitumour effect against a broad variety of tumour cell lines, such as melanoma, mesothelioma, prostate, breast lung and myeloma cancer cells in vitro.[6] The direct growth inhibitory effects have been attributed to cell cycle arrest and/or induction of apoptosis. It has been shown that nitrogen-containing bisphosphonates such as Alendronate and Zoledronate, act by inhibiting the mevalonate pathway.[7-8] Numerous studies have also described their ability to inhibit tumour cell adhesion and invasion but the mechanism is still unclear.[9] However, the major drawback of these drugs resides in their poor bioavailability mainly due to their preferential accumulation in bone. In order to enhance the antitumour activity of BPs, various strategies are used: development of BPs analogues with a lower bone mineral affinity[10], encapsulation in liposomes...[11] An other strategy is the vectorization through nanocrystal functionalization. In previous work,[12] γFe_2O_3 nanocrystal was surface functionalized with HMBP-$(CH_2)_3$–COOH.

We have shown that HMBP groups are highly complexing agent for iron oxide nanocrystal surface[12]. In this study, we used this high iron affinity to coat the nanocrystal surface with three HMBPs: Zoledronate (HMBP-(CH_2)- ), Alendronate (HMBP-$(CH_2)_3$–NH_3^+) and Neridronate (HMBP-$(CH_2)_5$–NH_3^+) which have no anti-osteoclastic properties. The antitumour activity of free HMBPs and HMBPs coated nanocrystals is evaluated in vitro and compared using MDA-MB-231 breast cancer cells as cell models.

The maghemite γFe_2O_3 nanocrystals were synthesized and surface functionalized according to a procedure already described.[12] The passivation process is performed in acidic media. The HMBPs coated particles were collected under magnetic field and washed three times with acidic water. The recovered nanoparticles were then dispersed in distilled water. The TEM images (inserts Figure 1) of deposited nanocrystals indicate an average diameter and a size distribution respectively equal to 10 nm and 20%, as observed in previous work.[12] Nanocrystal surface characterization is performed with FTIR and ^{31}P NMR spectroscopies. Comparing the FTIR spectra (Figure 1) of γFe_2O_3@HMBP nanocrystals (red curve) with the free HMBP solution (blue curve), large changes are observed within the P-O stretching region (1200-900 cm^{-1}) whereas amine vibration band (1600 cm^{-1}) for Alendronate (Figure 1A) and Neridronate (Figure 1B) and the imine vibration band (1650 cm^{-1}) for Zoledronate (Figure 1C) are unchanged. These results are in agreement with previous work and indicate that HMBPs are grafted onto the nanocrystal surface through the phosphonate groups.[12] Hence, comparing more conventional coating agents, the HMBP groups appear more highly complexant for iron oxide surface than carboxylic or amine functions.

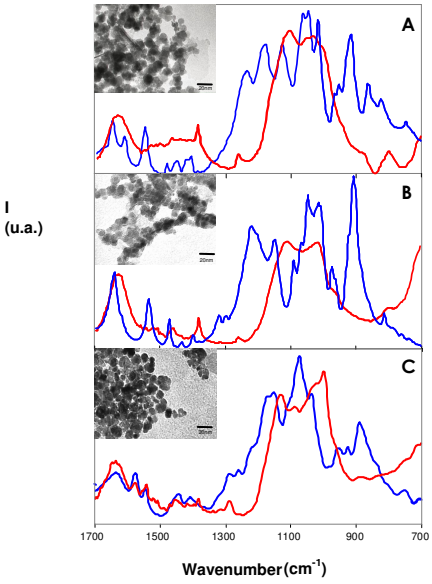

Figure 1: FTIR spectroscopy in KBr pellets: free HMBPs molecules (blue curve), γFe_2O_3@HMBPs (red curve) (A) Alendronate ; (B) Neridronate; (C) Zoledronate

To quantify the average number of molecules per nanocrystal ^{31}P NMR spectroscopy is used. A calibrate curve is established using free solution of HMBPs at various concentration in presence of an intern reference NaH_2PO_4 (10^{-1} $mol.L^{-1}$; NMR ^{31}P {^1H} (80.9 MHz): 0 ppm). After chemical decomposition of the magnetic γFe_2O_3@HMBP nanocrystals in acidic medium (nitric acid 65%), the ferrous ions are precipitated by addition of sodium hydroxide NaOH (10^{-1} $mol.L^{-1}$) in order to avoid switching of the ^{31}P NMR signal. The supernatant is analyzed with ^{31}P NMR and the concentration (number of molecules per nanocrystal) of HMBP into the sample is deduced from this calibration curve. (Alendronate: NMR ^{31}P {1H} (80.9 MHz): 17.076 ppm; Neridronate: NMR ^{31}P {1H} (80.9 MHz): 18.322 ppm; Zoledronate : NMR ^{31}P {1H} (80.9 MHz): 15.36 ppm). An average number of 550 ± 50 molecules per nanoparticle is obtained for γFe_2O_3@Zoledronate and 490 +/- 60 molecules is obtained for Alendronate coated nanocrystals. Whereas this number decreases to 250 +/- 40 for particles coated with Neridronate (Table 1).

	γFe_2O_3@Alendronate	γFe_2O_3@Neridronate	γFe_2O_3@Zoledronate
N/particle	490+/- 60	250+/- 40	550+/- 50
pH	4-12	6-12	3-12
Z (mV)	-12.8	-25.3	-21.6
Z/N	-0.026	-0.101	-0.058

Table 1: Average number of HMBP molecules per particle, pH range stability and zeta potential (Z)

This decrease in coverage density could be explained taking into account of the spacer between HMBP and amine groups. By increasing the alkyl chain length (comparing Alendronate to Neridronate), the flexibility of the chain increase, favouring interaction between one phosphonate and NH_3^+ groups. This induces steric hindrance and relatively disordered structure at the nanocrystal surface. Such behavior has been well demonstrated modelling the interaction of Alendronate and Neridronate with hydroxyapatite surface ($Ca_{10}(PO_4)_6(OH)_2$).[13] It has been shown that the Neridronate interacts less effectively than Alendronate because the long amino side chain folds in on itself with the formation of hydrogen bond between the amino group and one phosphonate group (Schema 2 A and B). So Neridronate does not align with the surface of the mineral. It is reasonable to assume that the instability observed for the interaction of Neridronate with calcium ions is valid for iron ions from the γFe_2O_3 nanocrystal surface.

This behaviour is also supported taking into account of one hand of pH range stability and on other hand of average charge surface of γFe_2O_3@HMBPs nanocrystals (Table 1). The γFe_2O_3@HMBPs nanocrystals are stable

at physiological pH, however the pH range stability is dependant of the coating agent. HMBPs are highly charged molecules, with five pKa values (Table 2). Considering, that HMBPs coordinate to iron surface via two Fe-O-P bonds (corresponding to pK_{a1} and pK_{a2}), the γFe_2O_3@Neridronate nanocrystals are only stable above pK_{a3} because at this pH the deprotonation of the third hydroxyl group occurs. Below pH 6, the charge is globally neutral due to the hydrogen bonding between NH_3^+ and the P-O group (Scheme 2 B).

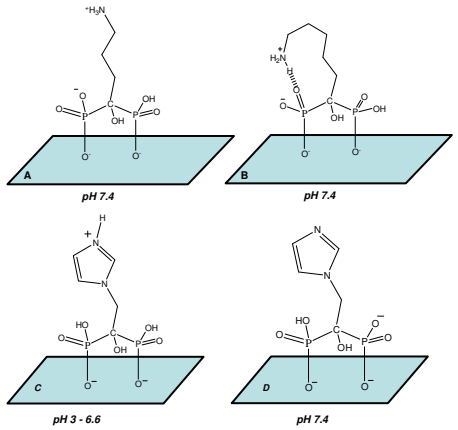

Scheme 2: Proposed structure of Alendronate (A), Neridronate (B) interacting on γFe_2O_3 nanocrystals surface at physiological pH and Zoledronate interacting on γFe_2O_3 nanocrystals surface at pH 3-6.6 (C) and at physiological pH (D)

	Pka_1	Pka_2	Pka_3	Pka_4	R_2 Functional group
Alendronate	~0.8	2.07	6.10	10.50	Amine 11.41
Neridronate	~0.8	2.36	6.43	10.86	Amine 11.21
Zoledronate	~0.8	2.89	6.63	10.99	1-H imidazole 6.95

Table 2: pKa of the HMBPs

At physiological pH, the γFe_2O_3@HMBPs particles exhibit a negative zeta potential (Table 1). Taking into account of the previous considerations, at pH 7.4, phosphonate protons dissociate leading to increased concentrations of monoprotonated species of all the bisphosphonates. At this pH, the amine of Alendronate and Neridronate is protonated. In the case of Neridronate, the amine interacts strongly with P-O (Schema 2B). Therefore, the hydrogen bonding between NH_3^+ and the P-O group expected within the Neridronate molecule induces a more negative zeta potential for γFe_2O_3@Neridronate than for γFe_2O_3@Alendronate which presents an effective NH_3^+ positive charge. For Zoledronate, under pH=3 surface coordination is not highly efficient to stabilize nanoparticles. Between pH=3 and 6.6, it can be expected that stability is induced by electrostatic repulsion between nanocrystals via the protonated nitrogen of the imidazol (Scheme 2C). At pH=7.4, the H-imidazole is deprotonated and phosphonate protons dissociate leading to increased concentrations of monoprotonated species (Scheme 2D). The average charge surface at physiological pH is then globally negative.

Free HMBP and the γFe_2O_3@HMBP nanocrystals were incubated with MDA-MB231 breast cancer cells for various extra cellular HMBP concentrations up to 100 µM for 48h and 72h. In previous work[12], we have shown that γFe_2O_3 nanocrystal surface functionalized with HMBP-$(CH_2)_3$–COOH are internalized following the endocytosis pathway and concentrate within intracellular vesicules (endosomes). As shown in Figure 2, γFe_2O_3@HMBP nanocrystals uptake by cells is well visualized by phase contrast optical microscope after Prussian blue staining. The experiments are performed for an equal concentration in HMBP (10 µM). Considering the average number of molecules per nanoparticle (table 1), the iron concentration for γFe_2O_3@Neridronate is twice compared to γFe_2O_3@Alendronate and γFe_2O_3@Zoledronate. Hence the number of nanocrystals into cells appears more important for γFe_2O_3@Neridronate (Fig 2 B).

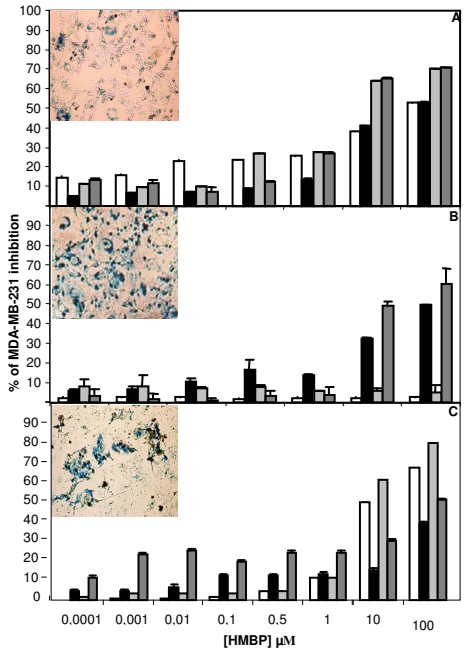

Figure 2: Comparative effects on MDA-MB-231 cell proliferation after different time of incubation of free HMBP (□ 48h, ▨ 72h) and γFe_2O_3@HMBP nanocrystals (■ 48h, ▩72h). A: Alendronate, (B) Neridronate, and (C) Inserts Optical images of mammal cell (MDA-MB-231) stained by Prussian blue and incubated with

γFe_2O_3@HMBP for 48h and corresponding to 0.01 mM in HMBP, showing nanocrystals incorporation into cells.

Figure 2 A shows that Alendronate and γFe_2O_3@Alendronate induce a similar concentration related and time dependant reduction in cell viability (IC50=100µM at 48 h). The behaviour of Neridronate and γFe_2O_3@Neridronate is clearly different (Figure 2B). In particular, Neridronate exhibits no inhibitory effect within the concentration range for 48h and 72h treatment. However, in presence of γFe_2O_3@Neridronate, cell viability is considerably reduced above 10 µM. Hence, The IC50 after 48 h is found equal to 100 µM and decrease at 10 µM after 72H. This clearly indicates that Neridronate cell penetration is induced by nanocrystal vectorization through γFe_2O_3 surface functionalisation. Cellular tests performed on MDA-MB231 indicate no cytoxicity for γFe_2O_3. For free Zoledronate the IC50 at 48h is achieved to a concentration of $10\mu mol.L^{-1}$ while for γFe_2O_3@Zoledronate it is at $100\mu mol.L^{-1}$. Hence, the activity of free Zoledronate is more important than γFe_2O_3@Zoledronate. However such results indicate that Zoledronate vectorization into cells through nanocrystal surface functionalization can be achieved in order to target selectively malignant cells. To increase γFe_2O_3@Zoledronate nanocrystals cell internalization, a magnetic field can be applied during the incubation. Magnetofection is a simple and highly efficient transfection method that uses magnetic fields to concentrate particles into the target cells. When a magnetic field is applied, cell viability is considerably reduced in presence of γFe_2O_3@Zoledronate. Hence, at 100 µmol.L under an applied of magnetic field, proliferation decrease to 75 % compared to 40 % without magnetic field. In this way, the magnetic force allows a very rapid concentration of the entire applied vector dose onto cells, so that 100% of the cells get in contact with a significant vector dose. The magnetic particles are then concentrated on the target cells by the influence of the external magnetic field generated by magnets. The cellular uptake of the particles is accomplished by endocytosis, natural biological processes. Consequently, membrane architecture and structure stay intact, in contrast to other physical transfection methods that damage the cell membrane.

Hence, results obtained with γFe_2O_3@HMBPs clearly indicate that inhibitory effect on cells proliferation is induced by drugs after nanocrystal cell internalization.

The mechanism of drugs action or drug release is not demonstrated here. However the anchoring to the nanoparticle's surface allowed to increase their hydrophobicity and also to change the therapeutic target, increasing the HMBP intestinal absorption instead of their accumulation in bone.

As a conclusion, we designed new antitumour magnetic nanoparticles by coating iron oxide nanoparticles with clinical anticancer molecules: Alendronate and Zoledronate. We show that the nanoparticle functionalization improves the Neridronate cell penetration and their antitumour effect. For Zoledronate, The activity is slightly less important than free molecules but increase considerably with magnetotransfection. These results allow us to consider these nanohybrid particles as a drug delivery system. Hence, we expect to improve these specific molecules targeting, and then their in vivo antitumour effect, by decreasing their natural accumulation in bone and using magnetic force targeting. For this purpose, in vivo experiments are in progress to evaluate the antitumour potency of γFe_2O_3@HMBP nanocrystals. In addition, the γFe_2O_3 core could be used as MRI contrast agent[12] for a good therapeutic evaluation.

1. J.R. Green, Cancer, 97, 840-847, 2003.
2. T.J. Martin, V. Grin, Australian Prescriber, 23, 130-132, 2000.
3. J.R. Green, M.J. Rogers, Drug Dev. Res., 55, 210–224, 2002.
4. G.H. Nancollasa, R. Tanga, R.J. Phippsb, Z. Hennemana, S. Guldea, W. Wua, A. Mangooda, R.G.G. Russellc, F.H. Ebetinob, Bone, 38, 617-627, 2006.
5. R. Graham, G. Russell, Bone, 40, S21-S25, 2007.
6. V. Stresing, F. Daubiné, I. Benzaid, H. Monkkonen, P. Clézardin, Cancer Letters, 257, 16-35, 2007.
7. M.A. Merell, S. Wakchoure, P.P.nlehenkari, K.W. Harris, K.S. Selander, European journal of pharmacology, 570, 27-37, 2007.
8. D. Ribatti, B. Nico, D. Mangieri , N. Maruotti , V. Longo , A. Vacca , F.P. Cantatore, Clinical Rheumatollogy, 26, 1094–1098, 2007.
9. K. Hashimoto, K.I. Morishige, K. Sawada, M. Tahara, S. Shimizu, S.I. Ogata, M. Sakata, K. Tasaka, T. Kimura, Biochemical and biophysical research communications, 354, 478-484, 2007.
10. S. Boissier, M. Ferreras, O. Peyruchaud, S. Magnetto, F.H. Ebetino , M. Colombel, P. Delmas, J.M. Delaissé, P. Clézardin, Cancer Research, 60, 2949–2954, 2000.
11. S.M. Zeisberger, B. Odermatt, C. Marty, A.H.M. Zehnder-Fjällman, K. Ballmer-Hofer, R.A. Schwendener, British Journal of Cancer, 95, 272–281, 2006.
12. Y. Lalatonne, C. Paris, J. M. Serfaty, P. Weinmann, M. Lecouvey, L. Motte, Chemical Communications, 22, 2553-2555, 2008.
13. J. Robinson, I. Cukrowski, H. M. Marques, Journal of Molecular Structur, 825, 134-142, 2006.